

Electronic Supplementary Information

Heterotelechelic Poly(propylene oxide) as Migration-Inhibited Toughening Agent in Hot Lithography Based Additive Manufacturing

Daniel Grunenberg,^a Katharina Ehrmann,^a Christian Gorsche,^{a,b} Bernhard Steyrer,^c Thomas Koch,^c Jürgen Stampfl,^c and Robert Liska^{*a}

^a Institute of Applied Synthetic Chemistry, Technische Universität Wien, Getreidemarkt 9/163-MC, 1060 Vienna (Austria)

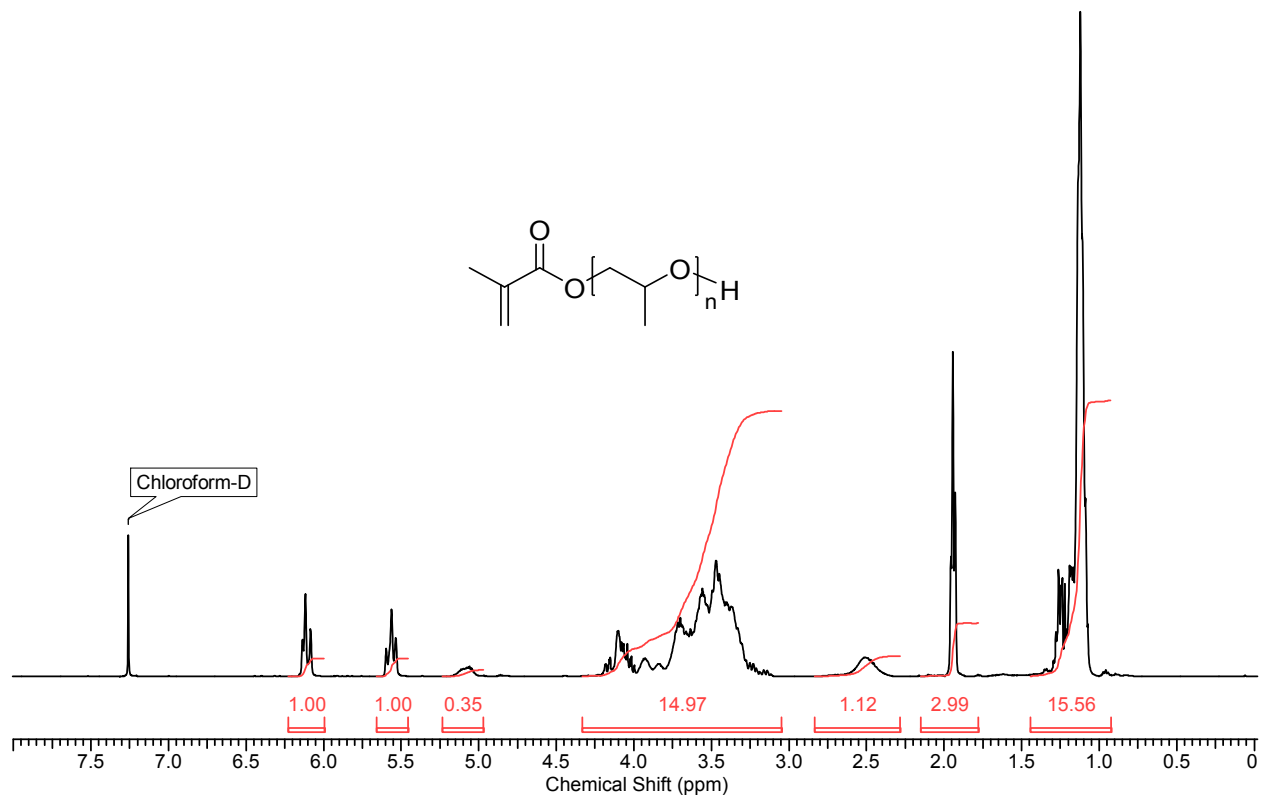
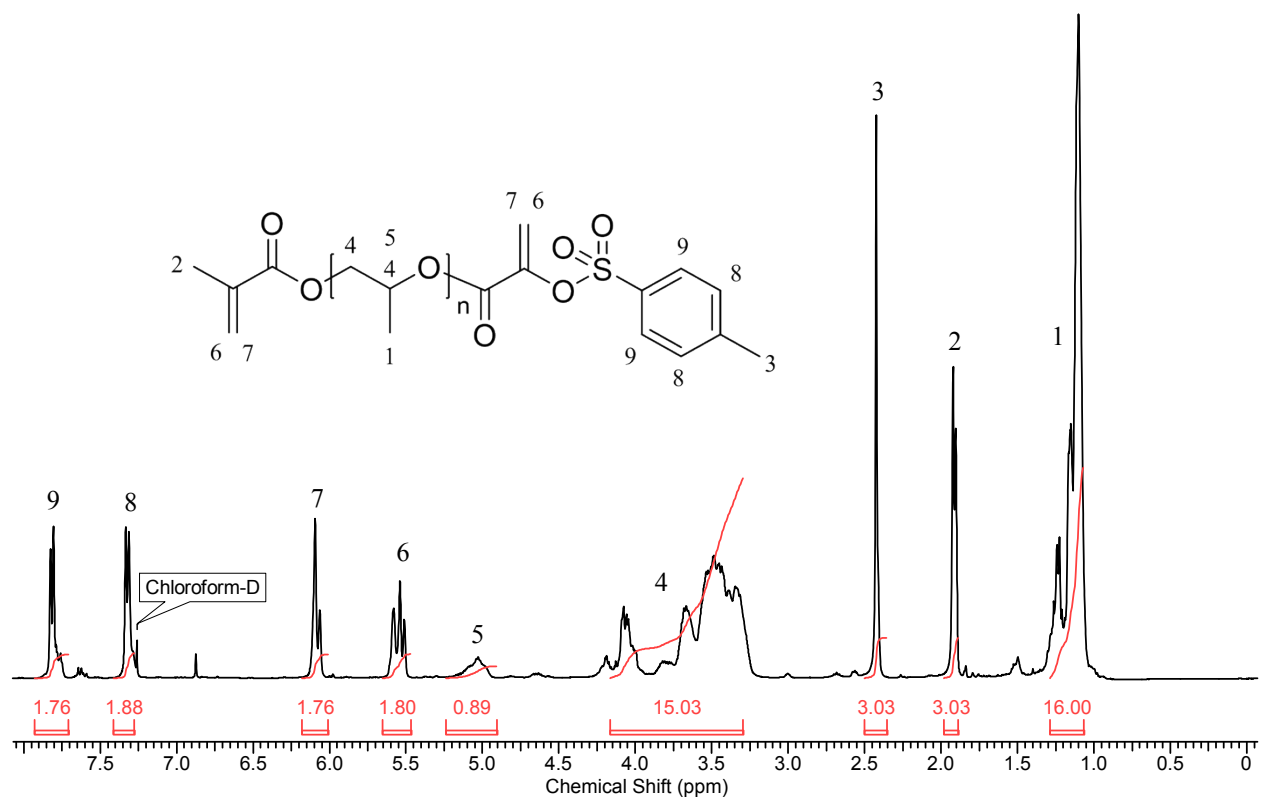
^b Cubicure GmbH, Gutheil-Schoder-Gasse 17, Tech Park Vienna (TPV), 1230 Vienna (Austria)

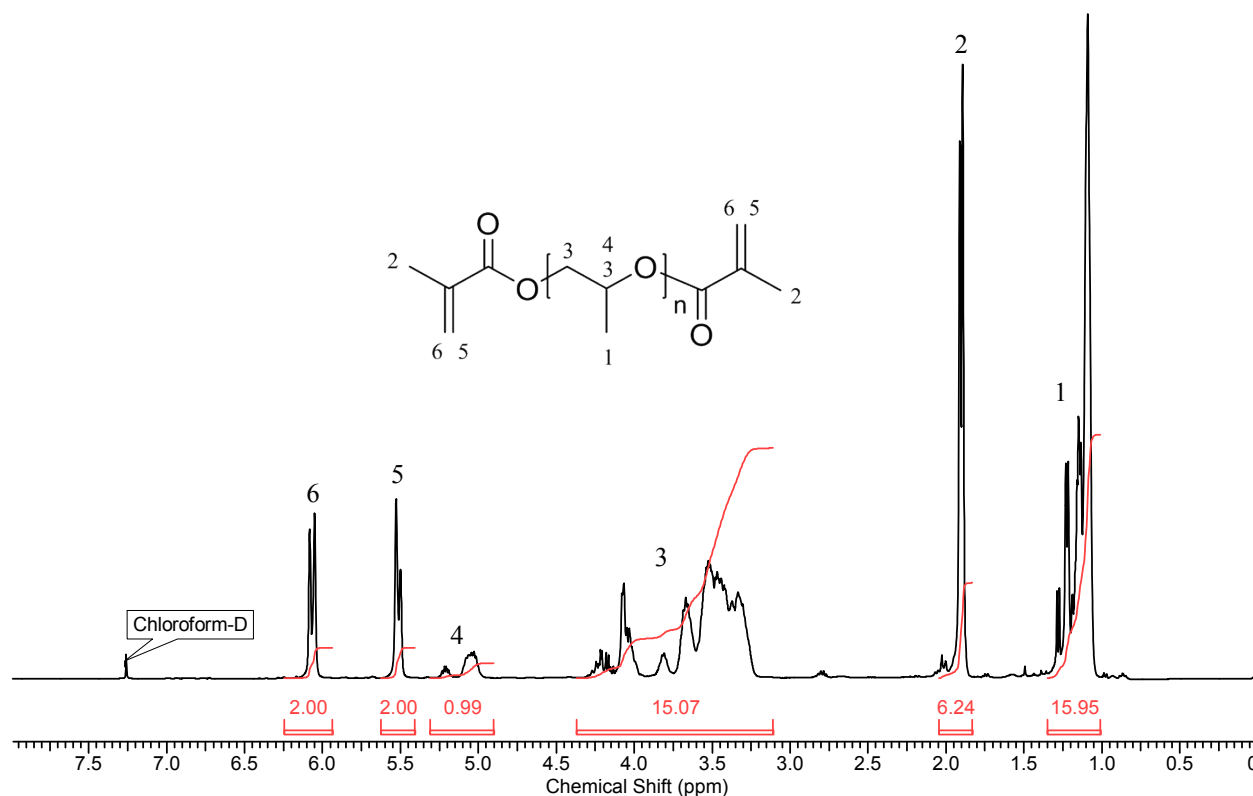
^c Institute of Materials Science and Technology, Technische Universität Wien, Getreidemarkt 9/308, 1060 Vienna (Austria)

Contents

1. NMR Analyses of Synthesized Oligomers.....	S2
2. Side Reaction of Tosyl Chloride and Hydrochinone.....	S3
3. DMTA, Tensile Testing, Dynstat, and Swelling Data.....	S4
4. Image of the Printed Specimens for DMTA, Tensile Testing, and Dynstat.....	S5

1. NMR Analyses of Synthesized Oligomers

Figure S1: 400 MHz ¹H NMR spectrum of the starting material Bisomer PPM 5 LI.Figure S2: 400 MHz ¹H NMR spectrum of PPO Hybrid (PPO-H).

Figure S3: 400 MHz ¹H NMR spectrum of PPO Dimethacrylate (PPO-D).

2. Side Reaction of Tosyl Chloride and Hydroquinone

Previous experiments showed that for the synthesis of PPO-H, concentrated sulfuric acid was the most efficient transesterification catalyst. However, 3 wt% of hydroquinone had to be used in order to prevent premature polymerization. As the hydroquinone was hard to remove after the first reaction step, 1,4-Phenylene bis(4-methylbenzenesulfonate) was formed as a side product during the second reaction step. Most of the side product could be removed during workup. Nevertheless, traces can still be seen in the ¹H NMR spectrum of PPO-H.

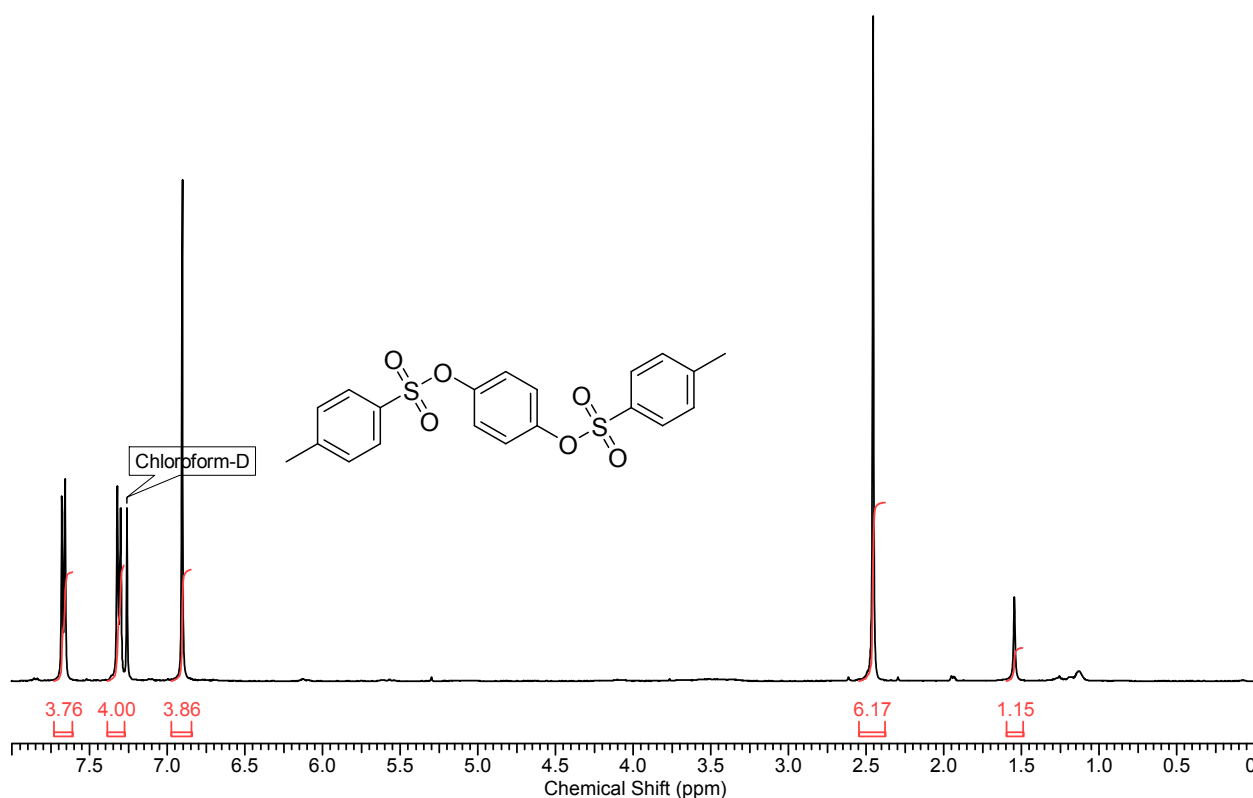


Figure S4: 400 MHz ¹H NMR spectrum of 1,4-Phenylene bis(4-methylbenzenesulfonate) as the side product during PPO-H synthesis.

3. DMTA, Tensile Testing, Dynstat, and Swelling Data

In the following table, data obtained from DMTA, tensile tests, dynstat experiments, and swelling experiments discussed and depicted in Figures 2-5 and 7-10 in the paper are given. Figure S5 displays representative stress-strain curves of all discussed materials.

Table S1: Thermomechanical characteristics for moulded and 3D printed specimens made from pure Bomar and Bomar with 10 - 25 db% poly(propylene oxide) dimethacrylate (PPO-D) or poly(propylene oxide) hybrid monomer (PPO-H): DMTA results (glass transition temperature (T_g), storage moduli at 25 °C (G'_{25} , as a measure for the onset of storage modulus decrease) and at the rubber plateau (G'_{rubber})); tensile testing results (ultimate tensile stress (σ_M), strain at break (ϵ_B), and energy at break (E_B , calculated from the area under the stress-strain curve)); impact strength (a) obtained from dynstat measurements; : swellability (S) and gel fraction (G)

Formulation	$T_g / ^\circ\text{C}^1$	G'_{25} / Pa^2	$G'_{rubber} / \text{Pa}^3$	σ_M [MPa]	ϵ_B [%]	E_B [MJ m ⁻³]	a [kJ m ⁻²]	S [%]	G [%]
Bomar	109	$1.79 \cdot 10^9$	$1.30 \cdot 10^7$	76.0 ± 2.2	14.3 ± 4.2	8.1 ± 2.7	12.7 ± 4.1	123^4	100^4
PPO-D "10 %"	102	$1.56 \cdot 10^9$	$1.36 \cdot 10^7$	70.9 ± 2.3	17.3 ± 6.3	9.5 ± 3.8	14.5 ± 3.1	123 ± 1	100^4
PPO-D "15 %"	101	$1.53 \cdot 10^9$	$1.54 \cdot 10^7$	66.8 ± 2.6	19.2 ± 7.6	9.2 ± 3.9	14.4 ± 5.0	122^4	99^4
PPO-D "20 %"	101	$1.42 \cdot 10^9$	$1.73 \cdot 10^7$	61.0 ± 2.2	17.7 ± 5.1	8.6 ± 2.9	15.3 ± 3.2	121^4	99^4
PPO-D "25 %"	99	$1.15 \cdot 10^9$	$1.70 \cdot 10^7$	55.5 ± 3.2	14.7 ± 6.6	6.6 ± 3.5	15.2 ± 1.4	120 ± 1	99^4
PPO-H 10 %	86	$1.50 \cdot 10^9$	$7.85 \cdot 10^6$	63.0 ± 1.6	32 ± 17	15.1 ± 7.8	19.7 ± 3.7	130 ± 1	98^4
PPO-H 10 % 3D	88	$1.52 \cdot 10^9$	$8.94 \cdot 10^6$	59.0 ± 1.2	20.2 ± 5.1	9.0 ± 2.2	7.8 ± 1.0	126 ± 1	99^4
PPO-H 15 %	76	$1.33 \cdot 10^9$	$6.52 \cdot 10^6$	54.1 ± 1.6	54 ± 18	21.5 ± 7.5	24.4 ± 2.2	133^4	97^4
PPO-H 15 % 3D	78	$1.39 \cdot 10^9$	$7.47 \cdot 10^6$	50.5 ± 0.9	38 ± 17	14.1 ± 6.8	11.8 ± 4.1	128^4	99^4
PPO-H 20 %	66	$1.10 \cdot 10^9$	$5.35 \cdot 10^6$	43.0 ± 2.9	84 ± 14	30.0 ± 6.3	28.2 ± 2.1	139 ± 1	94 ± 1
PPO-H 25 %	55	$7.48 \cdot 10^9$	$4.05 \cdot 10^6$	34.7 ± 4.7	112 ± 16	29.2 ± 5.7	47.4 ± 6.1	154 ± 3	87 ± 2

¹ determined from the maximum of the loss factor curve

² first G' value at/after 25.0°C

³ mean of all G' values between 141 and 200 °C

⁴ deviation of triplicates < 0.5%

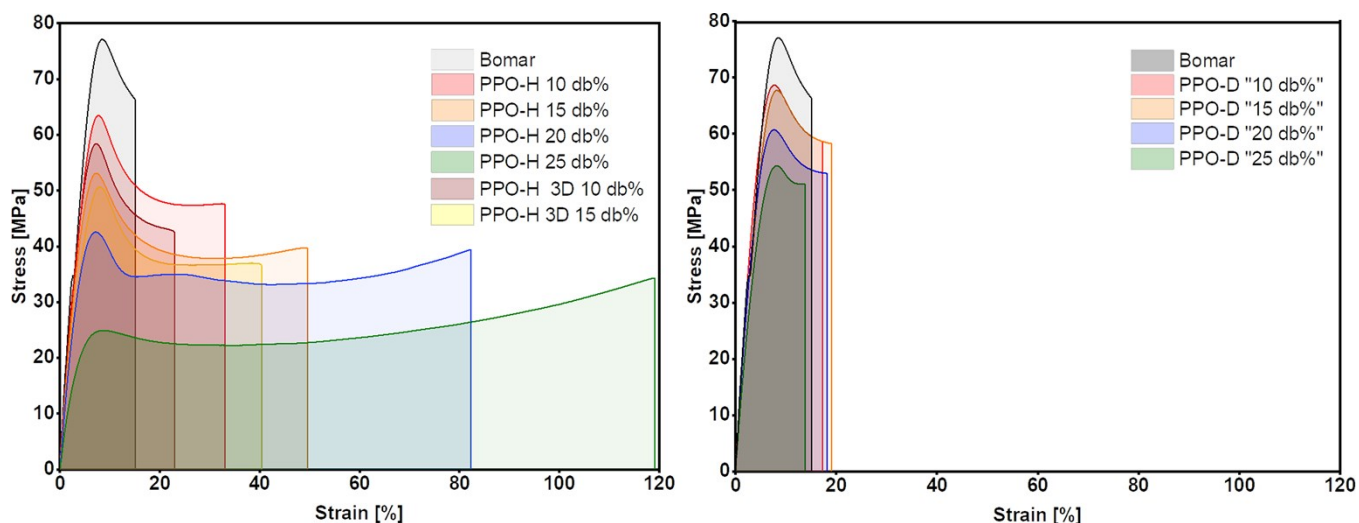


Figure S5: Representative stress-strain curves of PPO-H containing testing specimens (left) and PPO-D containing testing specimens (right) compared to only Bomar-containing testing specimens

4. Image of the Printed Specimens for DMTA, Tensile Testing, and Dynstat

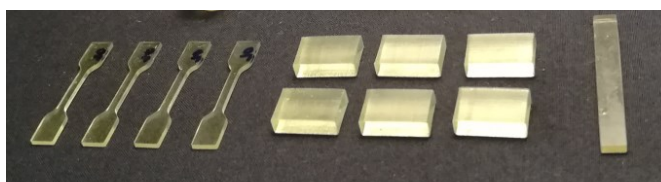


Figure S6: Image of the 3D-printed specimens for tensile testing (left), dynstat testing (middle), and DMTA (right)